Journal of Molecular Structure 1286 (2023) 135592

Contents lists available at ScienceDirect

Journal of Molecular Structure

journal homepage: www.elsevier.com/locate/molstr

Vibrational and ultrasonic relaxation spectroscopic study of keto-to-enol tautomerism: The case of acetylacetone

I.G. Karvounis [a], P. Siafarika [a], A.G. Kalampounias [a,b,*]

[a] Department of Chemistry, University of Ioannina, Ioannina, GR 45110, Greece
[b] University Research Center of Ioannina (URCI), Institute of Materials Science and Computing, Ioannina, Greece

ARTICLE INFO

Keywords:
Acetylacetone
B-diketones
Tautomerism
Raman
Ultrasonic relaxation spectroscopy

ABSTRACT

We report on a concentration-dependent Raman and ultrasonic relaxation study of the binary acetylacetone solutions in a wide mole fraction range. We combined vibrational and ultrasonic relaxation spectroscopies with DFT theoretical calculations for the systematic examination of the keto-to-enol tautomerism taking place in acetylacetone solutions with polar and non-polar solvent. Two sets of solutions were prepared with different solvents in terms of polarity. Raman spectra revealed that the keto and enol tautomers of acetylacetone coexist in solution and the keto tautomer is favored as the solvent polarity increases. A single Debye-type relaxation process is detected in the acoustic spectra, which is assigned to the interconversion process between ACAC tautomers. The isentropic volume change associated with the isomerization reaction was estimated from the acoustic data and found to decrease up to x∼0.2, while above this mole fraction reaches an almost constant value of ∼13.6 ml/mol, close to the theoretically estimated value of $\Delta V_{theor,CCl4}$=12.955 ml/mol in CCl_4 solvent environment. The keto-to-enol isomerization in the dilute region was found to be strongly affected by the presence of the non-polar solvent molecules, while for mole fractions higher than x∼0.3 the process is not considerably altered. Several physical properties of the system including density and acoustic properties, as well as the intermolecular free length and polarizability exhibited an inflection point at a specific mole fraction signifying the cross-over of two different regimes related with different tautomerization rates analogous to that observed in the Raman spectra. The results are analyzed and discussed in the framework of the current phenomenological status of the field.

1. Introduction

β-diketones are a subgroup of ketones that exhibit a keto-to-enol tautomerism, which involves the migration of a proton amongst two constitutional isomers. The first description of the intramolecular motion of beta carbonyls has been made by Courtot and Pichon [1–3]. Latter Lehn and Aprahamian have been synthesized and studied several beta carbonyls as rotary switches [4–6]. Recently, similar phototropic systems have been developed as proton cranes [7,8].

Acetylacetone (ACAC) is the simplest representative example of β-diketones and is considered as a model system for studying keto-to-enol tautomerization. It is a colorless organic liquid that is a precursor to a bidentate ligand, namely the acetylacetonate anion and is a building block for the synthesis of heterocyclic compounds [9]. Particularly, its enol form is utilized extensively in organic, inorganic, and medicinal syntheses [9]. Therefore, it is of interest to separate and isolate the tautomers. ACAC has attracted intensive research both experimentally [see e.g. 10–15] and theoretically [16–19]. Nevertheless, the keto-to-enol tautomerization ratio in different solvents and the structural characteristics of the tautomers are not entirely understood due to conflicting results. From the earlier studies it was proposed that, enol tautomers belong to a C_{2V}, symmetrical structure [14], but latter it was observed that it remains in a C_S symmetrical structure [15] as shown in Scheme 1.

Both keto and enol tautomers of acetylacetone coexist in solution and the keto tautomer is favored as the solvent polarity increases [10–19]. In Scheme 1, (a) and (b) are shown the two keto forms, with the (b) form to be expected at higher energies [20]. These two keto conformational species originate from the skeletal torsion relative to the planar structure. The (a) and (b) keto forms demonstrate C_2 and C_s symmetry, respectively. The enol tautomers of ACAC are favored in the gas phase and may exist in several forms as presented in Scheme 1 (c) to (f). The enol form with C_{2V} symmetry has a hydrogen atom shared equally between the two oxygen atoms [12]. The enol tautomers, presented in

* Corresponding author. Department of Chemistry, University of Ioannina, GR-45110 Ioannina, Greece.
E-mail address: akalamp@uoi.gr (A.G. Kalampounias).

https://doi.org/10.1016/j.molstruc.2023.135592
Received 24 January 2023; Received in revised form 5 April 2023; Accepted 16 April 2023
Available online 17 April 2023

Scheme 1 (d) and (e), contain a hydrogen bonded ring revealing two equivalent structures of C_s symmetry, while the structure (c) with C_{2V} symmetry indicates their transition state. The enolic form presented in Scheme 1 (f) corresponds to a higher energy structure. The two trans-enolic forms of ACAC presented in Scheme 1 (g) and (h), correspond to even higher energies due to the stabilizing attractive interaction between acetyl oxygen and the carbonyl carbon atom of the cis-acetate group.

In this work, we propose an alternative approach to investigate the keto-enol equilibrium in a solvent environment that alters the polarizability of the tautomeric forms of acetylacetone through intramolecular and intermolecular hydrogen bonding interactions. The effect of solvent polarity on the keto-to-enol tautomerism has been elucidated using Raman spectroscopy and computational methodologies. Density functional theory (DFT) calculations were performed to investigate the vibrational and thermodynamic properties of both tautomers of acetylacetone in both vacuum and solvent environment. A systematic concentration dependent study by means of ultrasonic relaxation spectroscopy has been undertaken for ACAC in solution state. The combined use of vibrational and acoustic spectroscopic tools with computational methodologies provides a promising approach to study tautomerization equilibrium. Ultrasonic techniques belong to the stationary relaxation techniques and their use depends on the frequency range of interest. These techniques cover the 10^4 to 10^{10} Hz frequency region, which means that one may perform relaxation times measurements in wide time scale, namely between 10^{-5} to 10^{-11} s. This so-wide time scale is difficult to be measured by a single spectroscopic technique (e.g. the corresponding time scale in vibrational spectroscopies is 10^{-12} to 10^{-14} s). Thus, acoustic techniques have been proved a powerful and less expensive tool in describing the dynamic picture of a molecular system [21–23] and references therein]. Furthermore, an additional advantage of ultrasonic techniques is that there are no restrictions on the type of processes that can be studied. Using Raman spectroscopy and analyzing changes in vibrational transition frequencies and spectral features of bands profiles (i.e. widths, intensities, moments, polarization properties) upon phase transformations, dilution, temperature and pressure changes, etc. one can provide a rather detailed description of microscopic interactions and dynamics of the system under study [24, 25]. On the other hand, the combination of vibrational and acoustic spectroscopies with computational methods has been proved a powerful and effective tool to identify hydrogen bonded structures shedding light on microstructural interactions. Except the experimental methods used in this work, other experimental and theoretical techniques have been used to study in detail the keto-to-enol isomerization [17,20,26–41] that strengthen and support the results of the present study.

2. Experimental

2.1. Preparation of solutions

Liquid acetylacetone (ACAC) with the chemical formula $CH_3COCH_2COCH_3$ was obtained from Merck (purity > 99%) and used without any further purification to prepare two sets of solutions with different solvents in terms of polarity. Carbon tetrachloride (CCl_4) was purchased from Sigma Aldrich (purity > 99%) and used as non-polar solvent. Ethanol (C_2H_5OH) was received from Merck (purity > 99.5%) and was used as polar solvent.

Solutions were prepared gravimetrically over a wide range of mole fractions. Dissolution of ACAC in each solvent was performed under continuous stirring at ambient conditions until a clear solution was received and correspond to mole fractions presented in Tables 1 and 2 of the Supporting Information.

2.2. Raman spectroscopy

Raman spectra were excited with the 532 nm laser-line of an air-cooled diode-pumped continuous wave laser (Excelsior series, Spectra-Physics). The Rayleigh scattering was eliminated by means of a notch filter permitting measurements close to the excitation line. The right-angle scattered light was analyzed by a single monochromator (IHR-320 JY, ISA-Horiba group) with a spectral resolution of 2 cm^{-1}. The system was equipped with a CCD detector thermoelectrically cooled to −70 °C for the signal detection. A VV polarization configuration, namely a vertical laser excitation and vertical analysis of scattered light, was used for recording the solution spectra. The laser power at the sample was below 50 mW to avoid heating the liquid. During the experiments, the optical geometry and the spectral slit width were kept constant. A CCl_4 reference sample was used to calibrate the polarization and correct

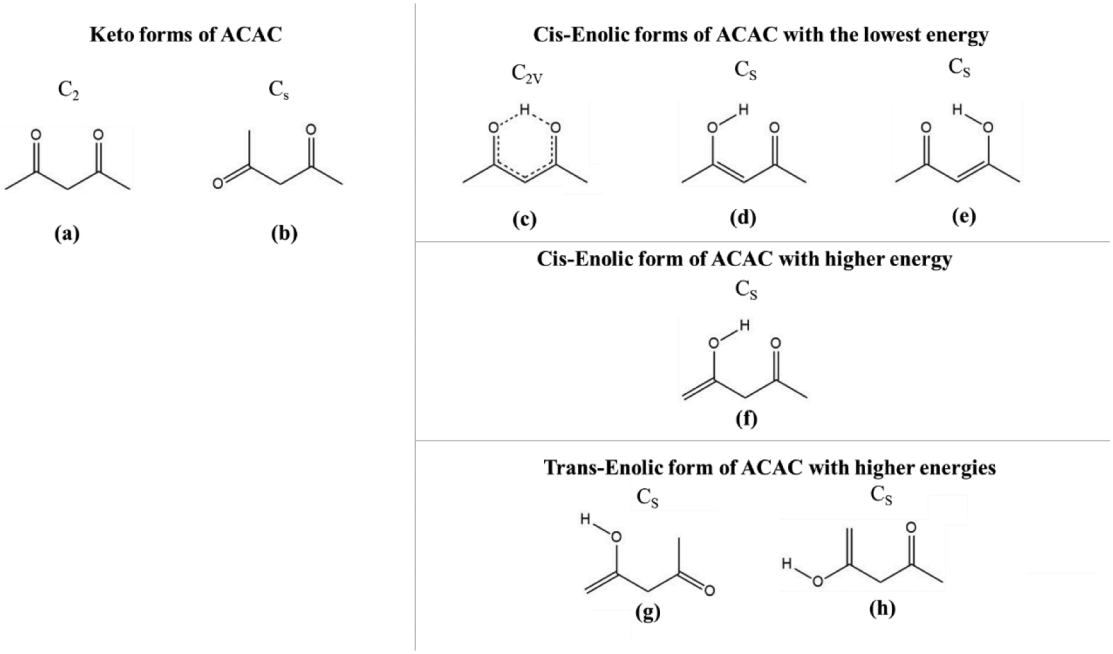

Scheme 1. The enol and keto tautomers of ACAC. Enolic forms may exist in cis- and trans-conformation. The symmetry of each species is also presented.

possible drifts of the monochromator's gratings. Accumulation times of several minutes were sufficient to result in a very high signal-to-noise ratio in the spectra. The Raman set up and the procedures for obtaining Raman have been described in detail elsewhere [42,43].

2.3. Ultrasonic relaxation spectroscopy

A pulse technique was used to measure the sound absorption coefficient. A set of two identical broad-band piezoelectric elements were used to send the signal to the sample and receive the transmitted signal after travelling a fixed distance of 1 cm. The repetition rate of the signal was set at 5 ms to avoid coincidence between the back wall echo-train and the subsequent pulse. All pulses were sampled 256 times and averaged with an oscilloscope (Tektronix, TBS 1202B) in the time-domain and then saved on a PC for further analysis. The attenuation in solutions is relatively high and therefore, the amplitude of the second echo is substantially lower than the amplitude of the first echo. The sound absorption coefficient of the solute as a function of frequency is estimated after subtracting the absorption of the solvent from that of the solution. The absorption of the CCl_4 solvent in the frequency range covered in this work is constant meaning that any relaxation effect attributed to solvent is absent. The experimental error for the sound absorption is ±0.01%.

A pulse-echo measurement scheme was used to measure the sound speed for all solutions. The difference in time-of-flight between the second and the first echo provides the speed of sound. The experimental error for the sound velocity is ±5%. The temperature for the acoustic cell was maintained constant at 20 °C within ±0.01 °C for all acoustic measurements. More details concerning the setup and the calibration procedure can be found elsewhere [44–46].

2.4. Density measurements

A density-meter (DMA 60, Anton Paar) was used to measure the solutions density with an uncertainty of ±0.0001 g/cm^3.

2.5. Quantum-mechanical calculations

The structure of the keto tautomer was received from the PubChem digital library of chemical compounds, while the enol tautomer was designed based on the structure of the keto tautomer. Density functional theory (DFT) method and specifically Becke's three parameter exchange functional [47] with the Lee–Yang–Parr correlation functional [48] (B3LYP) was used for all theoretical calculations with the 6–311++*G*(d, p) split-valance basis set that takes into account polarization and diffusion effects.

Optimization of the structures was carried out and new optimized atomic coordinates were obtained after energy minimization. The structure of the transition state was obtained from the optimized structures of the tautomers by means of the Synchronous Transit-Guided Quasi-Newton (STQN) method [49,50]. The thermodynamic properties and the vibrational frequencies for each normal mode for the structures of the two tautomers were calculated in the gas phase and in the presence of a homogeneous and isotropic environment, characterized by the dielectric properties of the corresponding solvent. No imaginary frequencies were received in the calculation of vibrational spectra. All calculations were performed utilizing the Gaussian 03 series of programs [51].

3. Results and discussion

3.1. Raman spectroscopy – structural properties

The following experimental verification of the solution speciation of the keto- and enol species by means of Raman spectroscopy complements the previous theoretical and experimental predictions and is of direct relevance to the aim of the present study. Fig. 1 shows the concentration dependence of Raman spectra obtained for xACAC-(1-x) Ethanol solutions with x denoting ACAC mole fraction. The spectra are interpreted in full agreement with the literature revealing gradual spectral variations [52–54]. The spectral features observed in Fig. 1 constitute a set of bands that are assigned as due to the ethanol and acetylacetone molecules and the spectra of the mixtures are a linear combination of the spectra of pure components. It seems that the presence of polar solvent molecules does not affect the keto-to-enol isomerization reaction.

The Raman spectrum of ethanol presented in Fig. 1 has eight typical characteristic bands. Starting from the low frequencies, the band at ~889 cm^{-1} is assigned to the CCO skeleton symmetric stretching vibration, the band at ~1055 cm^{-1} is related with the CO scaling and the band at ~1104 cm^{-1} is attributed to the CCO skeleton asymmetric stretching vibration. The bands observed at ~1287 and 1463 cm^{-1} are assigned to CH_2 and CH_3 antisymmetric deformation, respectively. In the high frequency region, the bands at ~2888, ~2934 and 2975 cm^{-1} are assigned to a superposition of the CH_3 and CH_2 symmetric stretching modes, to asymmetric CH_2 and asymmetric CH_3 modes [54 and references therein].

The Raman spectrum of acetylacetone is dominated by the intense polarized Raman line at ~2923 cm^{-1} that is assigned to the CH_3 symmetric stretching of the two methyl groups. The bands at ~3002 and ~2963 cm^{-1} are attributed to in plane and out of plane asymmetric CH_3 stretching mode, respectively [53,54]. The OH stretching modes of acetylacetone are extremely broad and almost featureless. The intense spectral envelop from 1600 to 1700 cm^{-1} is attributed to C = O, C = C stretching modes and to the CH in-plane bending mode [53,54]. The broadness of this strong band is probably related to the free rotation of the methyl group that is linked to the carbonyl functional group. This band splits into three components at low temperatures that are attributed to the co-existence of the two conformations [53].

The situation is different when ACAC is dissolved in a non-polar solvent as CCl_4. The concentration dependence of the xACAC-(1-x) CCl_4 solutions is presented in Fig. 2. In the dilute region with mole fraction ranging between 0.025 and 0.3, two newly appearing bands become evident in the Raman spectra near ~1550 and ~ 3600 cm^{-1} that are denoted in Fig. 2 with dotted lines. These bands are absent in the spectrum of pure solvent and thus are not attributed to CCl_4. The assembly of bands observed near ~1550 and ~ 3600 cm^{-1} in dilute region ($0.025 \leq x \leq 0.3$) gradually lose intensity upon further increase of the mole fraction. For $x > 0.3$, the spectra are almost identical with the spectra of xACAC-(1-x)Ethanol solutions for the same mole fraction. This means that the presence of non-polar solvent molecules affects significantly the keto-to-enol isomerization in the dilute region, while for mole fraction $x > 0.3$ the process is not considerably affected.

The Raman spectra shown in Figs. 1 and 2 will be discussed in relation to the theoretically predicted spectra of keto and enol forms of acetylacetone in an effort to elucidate the observed spectral peculiarities observed in dilute solutions with CCl_4. Fig. 3 shows Raman spectra obtained for pure ACAC and two representative Raman spectra of ACAC—CCl_4 solutions corresponding to $x = 0.075$ and $x = 0.4$ mole fractions. In Fig. 3 are also included the theoretically estimated Raman spectra of keto and enol form of ACAC for comparison. It is clearly seen that the two bands near ~1550 and ~ 3600 cm^{-1} observed in the Raman spectra of the dilute solutions are certainly assigned to the enol form on ACAC. Acetylacetone is converted to an enol acetate isomeric form in good yield in the presence of non-polar solvent (CCl_4) molecules. With increasing mole fraction of ACAC, the intensities of the ~1550 and ~ 3600 cm^{-1} bands show a gradual change indicating that the relative population between enol and keto isomeric forms reduces considerably, while above $x = 0.4$ varies with a completely different rate or remains almost unaffected. On the other hand, enolic acetylacetone exists in two forms, which interconvert by ultrafast reactions [54]. The preferred conformation of enol acetates of acetylacetone is the cis- and not the

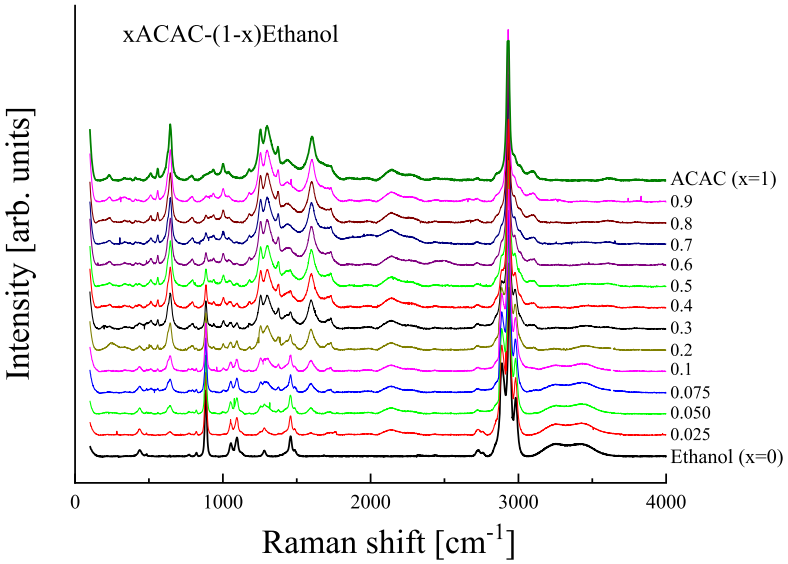

Fig. 1. Polarized (VV) Stokes-side Raman spectra of ACAC-Ethanol solutions for all mole fractions studied. The spectrum of pure solvent (ethanol) is also included for comparison. Spectral conditions: laser wavelength, $\lambda_0 = 532$ nm; laser power, $p = 50$ mW; spectral slit width, ssw= 2 cm^{-1}.

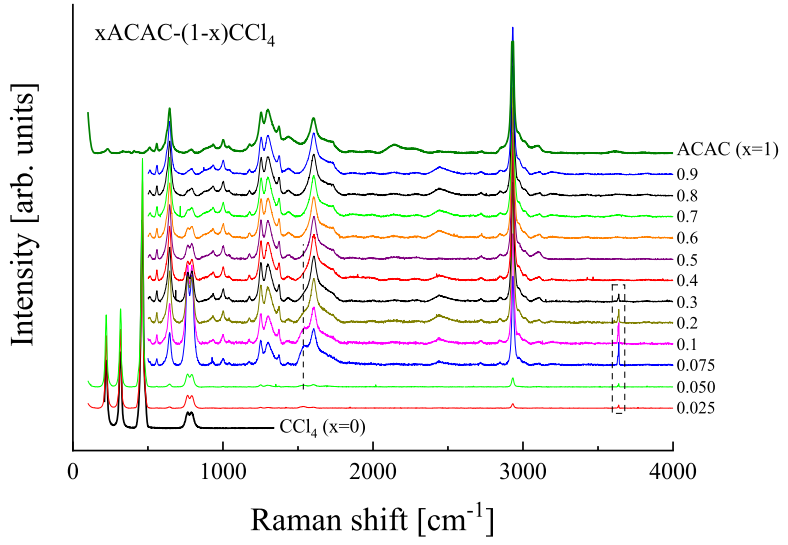

Fig. 2. Polarized (VV) Stokes-side Raman spectra of ACAC—CCl_4 solutions for all mole fractions studied. The spectrum of pure solvent (CCl_4) is also included for comparison. Spectral conditions: same as in Fig. 1.

trans-configuration due to the stabilizing attractive interaction between acetyl oxygen and the carbonyl carbon atom of the cis-acetate group. The fact that the non-polar solvent molecules significantly affect the keto-to-enol isomerization for $x<0.3$ are well documented in the literature cited in the Introduction, nevertheless the present study supports this finding through concentration-dependent Raman spectroscopy and ultrasonic relaxation. These two experimental methods are presented for the first time in the literature, constituting the novelty of this study.

3.2. *Ultrasonic relaxation spectroscopy – dynamic properties*

Since the most abrupt variations in the relative population between enol to keto isomeric forms are observed below $x \leq 0.3$ for the xACAC-(1-x)CCl_4 solutions (see Fig. 2), we restricted our ultrasonic relaxation study in this concentration region. The dispersion of the absorption coefficient detected in ACAC- CCl_4 solutions, is shown in Fig. 4. The absorption coefficient varies in the frequency region of relaxation according to the Debye-type single relaxation function [55]:

$$\frac{a}{f^2} = \frac{A}{1 + \left(\frac{f}{f_r}\right)^2} + B \tag{1}$$

where A, B and f_r correspond to the maximum contribution of the relaxation to a/f^2, the sum of the classical part of the absorption and the characteristic relaxation frequency.

Two relaxation processes are expected to be present in the acoustic spectra of ACAC solutions with CCl_4 that are attributed to the conformation of the two isomeric methyl enol ethers of acetylacetone and the keto-to-enol tautomerization. Nevertheless, only one relaxation process is detected in this frequency range. The relaxation parameters received from the fitting of this theoretical equation to the experimental points are presented in Fig. S1 of the Supporting Information. The fingerprint of a conformational change in the acoustic spectrum would be a relaxation amplitude monotonic increase and a constant relaxation frequency with increasing solution concentration [44,56–58]. The mole fraction dependence of the relaxation amplitude and frequency exhibits a

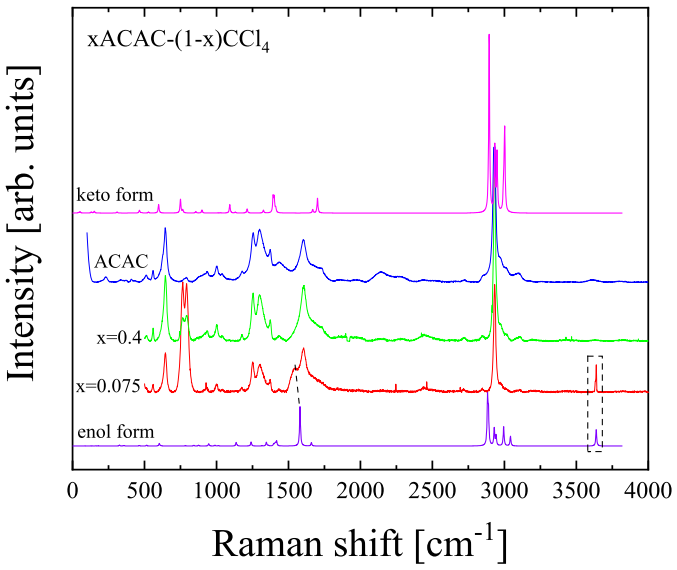

Fig. 3. Experimental Stokes-side Raman spectra of ACAC—CCl_4 solutions corresponding to $x = 0.075$ and 0.04 mol fraction and of pure ACAC. The calculated spectra of keto and enol conformers using CCl_4 as solvent are also shown for comparison. See text concerning calculation details.

completely different behavior. With increasing mole fraction, the characteristic frequency increases with a parallel relaxation amplitude decrease, while at x~0.2 an abrupt change is observed for both acoustic parameters. Therefore, we will analyze the experimental results along the line of interconversion process between ACAC tautomers. The monotonous behavior exhibited by f_r and A parameters up to $x = 0.2$ mole fraction is indicative of a continuous tautomerization process. The results do not directly show that the relaxation process is attributed to the ACAC tautomers' interconversion. At the most, it could be considered empirical.

In an effort to progress on the comprehensive understanding of the tautomerization process, we measured additional physical properties, namely the sound velocity and the density of the solutions covering a wide mole fraction region. The results are presented in Fig. 5(a) and (b), respectively in a semi-logarithmic representation. The specific representation permits the detection of an inflection point at a specific mole fraction for both physical properties of the system signifying the crossover of two different regimes that are related with different tautomerization rates similar to that observed in the Raman spectra of Fig. 2. It is well documented in the literature that the preferred conformation of enol acetates of acetylacetone is the *cis* form through experimental and computational methods and the present study supports this finding through concentration-dependent Raman spectroscopy and ultrasonic relaxation.

Another interesting parameter is the intermolecular free length L_f that describes the distance between surfaces of the molecules. This parameter can be estimated directly from the adiabatic compressibility of the system β_s, which is:

$$\beta_s = \frac{1}{\rho u^2} \tag{2}$$

where ρ is the mass density and u is the velocity of sound in the solutions. The intermolecular free length is estimated through the following empirical formula [59,60]:

$$L = K\sqrt{\beta_s} \tag{3}$$

where K is the so-called Jacobson's constant.

The calculated intermolecular free length L_f for all mole fractions is presented in Fig. 5(c). With increasing mole fraction under isobaric conditions, the intermolecular free length experiences a monotonous decrease, although with different tendencies below and above $x = 0.3$ mole fraction similar to that observed for sound velocity and density. The decrease indicates that the distance between neighboring molecules decreases with concentration enhancing the ultrasound wave propagation. This is reflected in the sound velocity measurements shown in Fig. 5(a). Molecular interactions are stronger at higher mole fractions forming a more rigid structure. It seems that the intermolecular free length is strongly related with sound velocity and mass density and may provide important information concerning not only intermolecular phenomena as molecular association, but also tautomerization processes.

3.3. Standard volume change associated to keto-to-enol tautomerism

The maximum value of the attenuation per cycle, μ_{max}, can be estimated from the sound velocity u, the amplitude of the relaxation A and

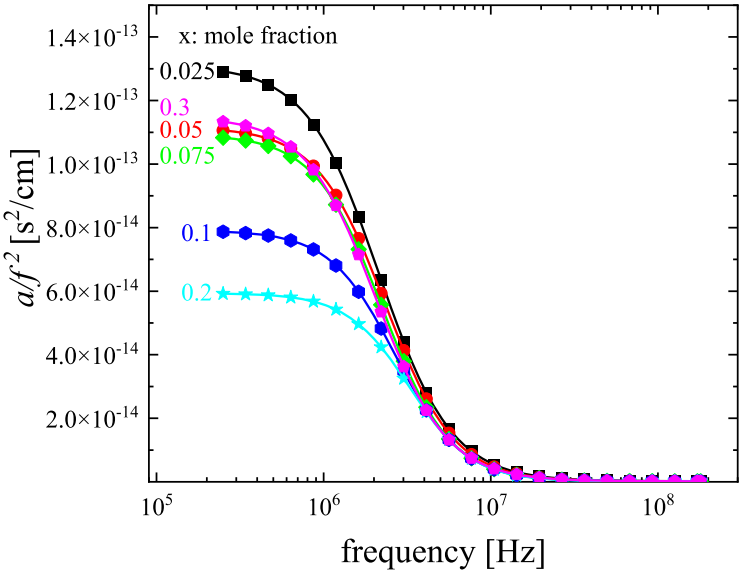

Fig. 4. Absorption spectra (α/f^2) of xACAC-(1-x)CCl_4 solutions at 20 °C. Solid lines represent the theoretical Debye-type profiles for each mole fraction. A single relaxation process is observed in this frequency range.

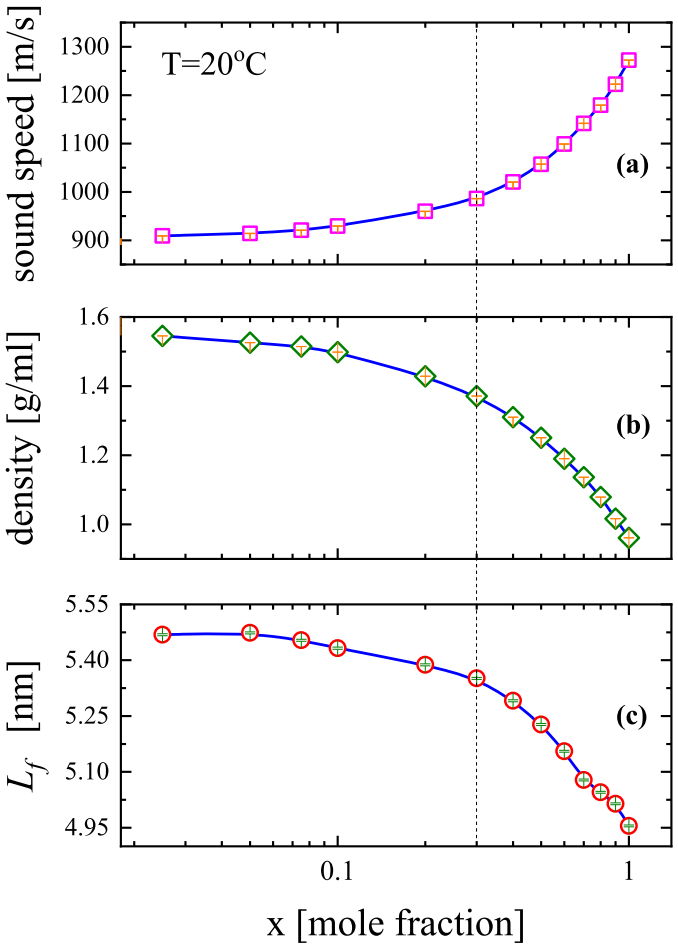

Fig. 5. Concentration dependence of the ultrasound velocity (a), density (b) and intermolecular free length (c) covering a wide mole fraction range. Acoustic parameters were measured at 20 °C. See text concerning the calculation of the intermolecular free length.

the characteristic relaxation frequency f_r through the equation [61]:

$$\mu_{max} = \frac{1}{2} A u f_r \tag{4}$$

The isentropic volume change ΔV_s associated with the isomerization process, depends on the maximum value of the attenuation per cycle according to [61]:

$$\Delta V_s = \sqrt{\frac{2RT\ \mu_{max}}{\pi \rho u^2 \Gamma}} \tag{5}$$

where ρ is the density of the solution, R is the gas constant and T is the absolute temperature. Finally, Γ is the concentration parameter, which is related with the progress of the isomerization reaction and is estimated as [62]:

$$\Gamma = \frac{1}{V}\left(\frac{\partial\left(\frac{n_i - n_i^0}{\nu_i}\right)}{\partial ln K_{eq}}\right)_{p,T} = C^0\left(\frac{\partial \beta}{\partial ln K_{eq}}\right)_{p,T} \tag{6}$$

where K_{eq} is the equilibrium constant and β denotes the dissociation degree. Parameter C^0 is the lower concentration limit where the material's response can be detected.

The so obtained isentropic volume change associated with the isomerization reaction as a function of mole fraction is presented in Fig. 6. The results reveal that the volume change decreases up to x~0.2 and above this mole fraction reaches an almost constant value of ~13.6 ml/mol, which is close to the theoretically estimated value of $\Delta V_{theor,CCl4}$=12.955 ml/mol considering CCl_4 solvent environment in the calculation model. The corresponding volume change in vacuum environment free of any intermolecular interactions was found equal to $\Delta V_{theor,vacuum}$=5.867 ml/mol and deviates significantly from the experimental value of the volume change. A greater deviation from the experimental value was observed when the theoretical calculations were carried out in ethanol solvent environment. In this case, the theoretical value of the volume change was found equal to $\Delta V_{theor,ethanol}$=3.858 ml/mol.

The transition state between the two minima corresponding to keto- and enol-isomers was estimated using the Synchronous Transit-Guided Quasi-Newton (STQN) method [49,50]. For the B3LYP/6–311++G(d, p) level of theory, we calculated the enthalpy change between isomers and the activation enthalpy in solvent environment equal to ΔH=5.86 kcal/mol and ΔH_a=53.40 kcal/mol, respectively. The corresponding values in vacuum are ΔH=5.84 kcal/mol and ΔH_a=53.19 kcal/mol, while the values are found equal to ΔH=6.03 kcal/mol and ΔH_a=53.87 kcal/mol in the case of ethanol solvent environment. Our calculated enthalpy difference is relatively close to the experimental value of ΔH_{exp}=4.66 kcal/mol reported in the literature [63], but rather higher compared to other theoretically estimated values reported in the past that where in the range 3.27 to 3.89 kcal/mol [64,65]. This deviation is probably due to the different level of theory used for the calculation by those authors. Furthermore, the activation enthalpy estimated in the present work is near to the 59.02 kcal/mol reported in the literature [64, 65].

3.4. Polarity effect on the tautomerization equilibrium

In keto-to-enol tautomerism, both tautomeric forms coexist in solution. Nevertheless, their relative amount depends on the solvent polarity, which strongly influences the equilibrium between the two tautomers. Polarity is an intrinsic molecular characteristic and describes the unequal distribution of electron density. In the context of Meyer's Rule, the keto tautomer is favored when the polarity of the solvent increases [66]. By comparing the polarity of the two tautomers, it seems that keto tautomer is more polar than enol due to the dipole-dipole repulsion induced by the two carbonyl functional groups present in the keto molecular structure. On the other hand, enol tautomer appears more stable than the keto form not only in solutions with non-polar

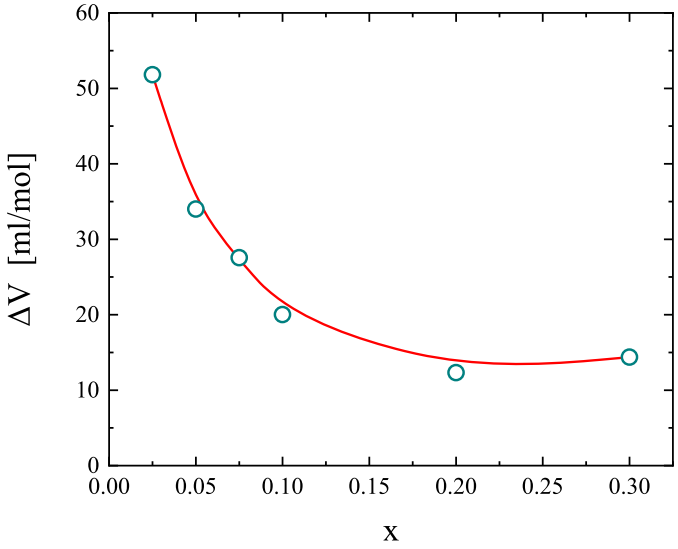

Fig. 6. Isentropic volume change for the keto-to-enol isomerization reaction as a function of solution concentration.

solvents, but also in the gas phase due to the resonance structure, forming a six-membered ring with the intramolecular hydrogen bond, which reduces the dipole-dipole interactions [66].

Polarity illustrates the permanent average separation of charge, while polarizability indicates the ability of a molecule to become polarized temporarily. Then based on the polarity of the molecule, polarizability provides information on how a specific molecule is affected when subjected to a dielectric medium. To quantitatively follow the effect of polarity on the tautomerization equilibrium and how the equilibrium changes as the solvent's polarity varies, we calculated the dielectric constant of a mixture at various polarizable conditions. In the context of the Onsager-Kirkwood theory, the polarizability of a given molecule within a dielectric medium is represented by the OK factor, as [67,68]:

$$OK = \frac{\varepsilon - 1}{2\varepsilon + 1} \tag{7}$$

where ε correspond to the dielectric constant of the mixture, which can be evaluated both experimentally [69,70] and theoretically [71]. The results are presented in Fig. 7 and reveal that the keto-to-enol tautomerism experiences a completely different behavior when placed in a highly polar and non-polar dielectric medium.

Interestingly, polarizability exhibits a gradual change with increasing ACAC mole fraction in ACAC—CCl_4 solutions analogous to that presented by all acoustic parameters and other physical properties of the system, indicating that the relative population between enol to keto isomeric forms reduces considerably although with different rates below and above x~0.2.

4. Conclusions

In this study, we combined vibrational and ultrasonic relaxation spectroscopies with DFT theoretical calculations for the systematic examination of the keto-enol tautomerism taking place in acetylacetone solutions with polar and non-polar solvent. The systematic analysis of the experimental and theoretical results revealed that the presence of non-polar solvent molecules affects significantly the keto-to-enol isomerization in the dilute region, while for mole fraction x>0.3 the process is unaffected. According to previous research works, acetylacetone is converted to an enol acetate isomeric form in the presence of non-polar solvent (CCl_4) molecules, while the preferred conformation of enol acetates of acetylacetone is the cis-form. The trans-configuration is not favored due to the stabilizing attractive interaction between acetyl oxygen and the carbonyl carbon atom of the cis-acetate group.

Only one relaxation process is detected that is attributed to the interconversion process between ACAC tautomers. The a/f^2 measurements were analyzed by means of a Debye-type distribution. The monotonous behavior exhibited by f_r and A parameters up to $x = 0.2$ mole fraction is indicative of a continuous tautomerization process. The semi-log representation reveals the presence of an inflection point at a specific mole fraction for both physical properties of the system signifying the cross-over of two different regimes that are related with different tautomerization rates like that observed in the Raman spectra.

The intermolecular free length experiences a monotonous decrease with increasing mole fraction, although with different tendencies below and above $x = 0.3$ mole fraction like that observed for sound velocity and density. The intermolecular free length parameter may provide important information concerning intermolecular association phenomena and tautomerization processes.

The isentropic volume change associated with the isomerization reaction decreases up to x~0.2 and above this mole fraction reaches an almost constant value of ~13.6 ml/mol, close to the theoretically estimated value of $\Delta V_{theor,CCl4}$=12.955 ml/mol in a CCl_4 solvent environment. Polarizability exhibits a gradual change with increasing ACAC mole fraction in ACAC—CCl_4 solutions analogous to that presented by all acoustic parameters and other physical properties of the system, indicating that the relative population between enol to keto isomeric forms reduces considerably although with different rates below and above x~0.2.

All the above findings can be practically attributed to the alterations in the network rigidity due to variations in interactions at molecular level. This study proves that the combination of Raman and ultrasonic relaxation spectroscopies with theoretical calculations is a powerful diagnostic tool for the adequate evaluation of the processes occurring in solutions. The elucidation of the detailed local structure is of key importance for the knowledge-based understanding of the structure and dynamics of ACAC solutions.

Declaration of Competing Interest

The authors declare that they have no known competing financial interests or personal relationships that could have appeared to influence the work reported in this paper.

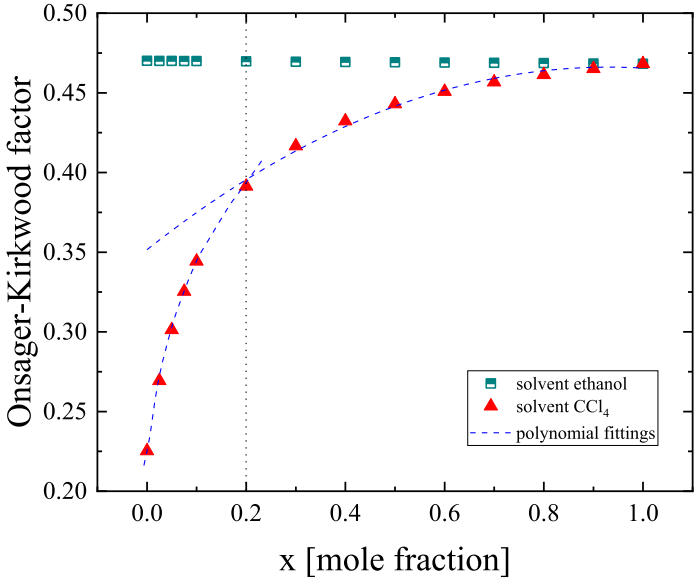

Fig. 7. Onsager-Kirkwood factor as a function of mole fraction. See text for more details concerning the calculation procedure.

Data availability

Data will be made available on request.

Acknowledgments

The authors greatly acknowledge Professor S. Boghosian, Department of Chemical Engineering, University of Patras, Patras, Greece, for providing access to macro-Raman facility. P. Siafarika acknowledges support by project "Dioni: Computing Infrastructure for Big-Data Processing and Analysis" (MIS No. 5047222) co-funded by European Union (ERDF) and Greece through Operational Program "Competitiveness, Entrepreneurship and Innovation", NSRF 2014–2020.

Supplementary materials

Supplementary material associated with this article can be found, in the online version, at doi:10.1016/j.molstruc.2023.135592.

References

[1] P. Courtot, R. Pichon, J.Le Saint, Tetrahedron Lett. 17 (1976) 1181.
[2] P. Courtot, R. Pichon, J.Le Saint, Tetrahedron Lett. 20 (1979) 1591.
[3] R. Pichon, J.Le Saint, P. Courtot, Tetrahedron 37 (1981) 1517.
[4] X. Su, I. Aprahamian, Org. Lett. 13 (2011) 30.
[5] H. Qian, I. Aprahamian, Chem. Commun. 51 (2015) 11158.
[6] M.N. Chaur, D. Collado, J.-.M. Lehn, Chem. Eur. J. 17 (2011) 248.
[7] K. Nakashima, A. Georgiev, D. Yordanov, Y. Matsushima, S. Hirashima, T. Miura, L. Antonov, J. Org. Chem. 87 (2022) 6794.
[8] K. Nakashima, A. Petek, Y. Hori, A. Georgiev, S. Hirashima, Y. Matsushima, D. Yordanov, T. Miura, L. Antonov, Chem. Eur. J. 27 (2021) 11559.
[9] T.M. Harris, 2,4-Pentanedione". 2,4-Pentanedione. e-EROS Encyclopedia of Reagents for Organic Synthesis, 2001.
[10] A.L. Andreassen, S.H. Bauer, J. Mol. Struct. 12 (1972) 381.
[11] M.M. Folkendt, B.E. Weiss-Lopez, J.P. Chauvel Jr, N.S. True, J. Phys. Chem. 89 (1985) 3347.
[12] N.S. Hush, M.K. Livett, J.B. Peel, G.D. Willett, Aust. J. Chem. 40 (1987) 599.
[13] K.A. Manbeck, N.C. Boaz, N.C. Bair, A.M.S. Sanders, A.L. Marsh, J. Chem. Educ. 88 (2011) 1444.
[14] A.H. Lowrey, C. George, P. D' Antonio, J. Karle, J. Amer. Chem. Soc. 93 (1971) 6399.
[15] R. Srinivasan, J.S. Feenstra, S.T. Park, S. Xu, A.H. Zewail, J. Amer. Chem. Soc. 126 (2004) 2266.
[16] S.H. Bauer, C.F. Wilcox, Chem. Phys. Lett. 279 (1997) 122.
[17] J. Mavri, J. Grdadolnik, J. Phys. Chem. A 105 (2001) 2039.
[18] O.A. Sharafeddin, K. Hinsen, T. Carrington Jr, B. Roux, J. Comput. Chem. 18 (1997) 1760.
[19] S.J. Grabowski, J. Phys. Org. Chem. 16 (2003) 797.
[20] J.J. Dannenberg, R. Rios, J. Phys. Chem. 98 (1994) 6714.
[21] G. Stogiannidis, S. Tsigoias, P. Mpourazanis, S. Boghosian, S. Kaziannis, A. G. Kalampounias, Chem. Phys. 522 (2019) 1.
[22] P. Siafarika, C. Kouderis, A.G. Kalampounias, Mol. Phys. 119 (2021), e1802075.
[23] C. Kouderis, P. Siafarika, A.G. Kalampounias, Polymer (Guildf) 217 (2021), 123479.
[24] C.B. Knudsen, A.G. Kalampounias, R. Rehrmann, S. Boghosian, J. Phys. Chem. B 112 (2008) 11996.
[25] A.G. Kalampounias, S.A. Kirillov, W. Steffen, S.N. Yannopoulos, J. Molec. Struct. 651-653 (2003) 475.
[26] S. Xu, S.T. Park, J.S. Feenstra, R. Srinivasan, A.H. Zewail, J. Phys. Chem. A 108 (2004) 6650.
[27] K. Iijima, A. Ohnogi, A. Shibata, J. Molec. Struct. 156 (1987) 111.
[28] Z. Yoshida, H. Ogoshi, T. Tokumitsu, Tetrahedron 26 (1970) 5691.
[29] A. Camerman, D. Mastropaolo, N. Camerman, J. Amer, Chem. Soc. 105 (1983) 1584.
[30] M.R. Johnson, N.H. Jones, A. Geis, A.J. Horsewill, H.P. Trommsdorff, J. Chem. Phys. 116 (2002) 5694.
[31] W. Egan, G. Gunnarsson, T.E. Bull, S. Forsen, J. Amer, Chem. Soc. 99 (1977) 4568.
[32] I. Adamovic, M.A. Freitag, M.S. Gordon, J. Phys. Chem. 118 (2003) 6725.
[33] S. Yamabe, N. Tsuchida, K. Miyajima, J. Phys. Chem. A 108 (2004) 2750.
[34] V.B. Delchev, Monatsh. Chem. 135 (2004) 249.
[35] W. Caminati, J.-.U. Grabow, J. Amer, Chem. Soc. 128 (2006) 854.
[36] N.V. Belova, H. Oberhammer, N.H. Trang, G.V. Girichev, J. Org. Chem. 79 (2014) 5412.
[37] I. Matanovic, N. Doslic, J. Phys. Chem. A 109 (2005) 4185.
[38] M.G. Giorgini, H. Torii, M. Musso, Phys. Chem. Chem. Phys. 2 (2010) 183.
[39] H. Wang, R. Liu, Y. Han, Y. Tan, S. Zhang, C. Jiang, X. Zheng, J. Molec. Liq. 337 (2021), 116436.
[40] Y. Han, R. Liu, C. Jiang, H. Wang, X. Zheng, J. Molec. Liq. 335 (2021), 116224.
[41] Z. Wang, K. Yu, Y. Zhao, J. Xue, C. Jiang, H. Wang, H. Wu, Spectrochim. Acta A Mol. Biomol. Spectrosc. 281 (2022), 121593.
[42] A.G. Kalampounias, G. Tsilomelekis, S. Boghosian, Mol. Phys. 110 (2012) 3095.
[43] A.G. Kalampounias, G. Tsilomelekis, S. Boghosian, J. Chem. Phys. 142 (2015), 154503.
[44] G. Stogiannidis, S. Tsigoias, A.G. Kalampounias, J. Mol. Liq. 302 (2020), 112519.
[45] A.G. Kalampounias, J. Mol. Struct. 1212 (2020), 128146.
[46] P. Mpourazanis, G. Stogiannidis, S. Tsigoias, G.N. Papatheodorou, A. G. Kalampounias, J. Phys. Chem. Solid. 125 (2019) 43.
[47] A.D. Becke, J. Chem. Phys. 98 (1993) 5648.
[48] C. Lee, W. Yang, R.G. Parr, Phys. Rev. B 37 (1988) 785.
[49] C. Peng, H.B. Schlegel, Israel J. Chem. 33 (1994) 449.
[50] C. Peng, P.Y. Ayala, H.B. Schlegel, M.J. Frisch, J. Comp. Chem. 17 (1996) 49.
[51] M.J. Frisch, G.W. Trucks, H.B. Schlegel, G.E. Scuseria, M.A. Robb, J.R. Cheeseman, G. Scalmani, V. Barone, G.A. Petersson, H. Nakatsuji, X. Li, M. Caricato, A. Marenich, J. Bloino, B.G. Janesko, R. Gomperts, B. Mennucci, H.P. Hratchian, J.V. Ortiz, A.F. Izmaylov, J.L. Sonnenberg, D. Williams-Young, F. Ding, F. Lipparini, F. Egidi, J. Goings, B. Peng, A. Petrone, T. Henderson, D. Ranasinghe, V.G. Zakrzewski, J. Gao, N. Rega, G. Zheng, W. Liang, M. Hada, M. Ehara, K. Toyota, R. Fukuda, J. Hasegawa, M. Ishida, T. Nakajima, Y. Honda, O. Kitao, H. Nakai, T. Vreven, K. Throssell, J.A. Montgomery Jr., J.E. Peralta, F. Ogliaro, M. Bearpark, J. J. Heyd, E. Brothers, K.N. Kudin, V.N. Staroverov, T. Keith, R. Kobayashi, J. Normand, K. Raghavachari, A. Rendell, J.C. Burant, S.S. Iyengar, J. Tomasi, M. Cossi, J.M. Millam, M. Klene, C. Adamo, R. Cammi, J.W. Ochterski, R.L. Martin, K. Morokuma, O. Farkas, J.B. Foresman, D.J. Fox, Gaussian 03, Revision A.02, Gaussian, Inc., Wallingford CT, 2003.
[52] A. Emin, A. Hushur, T. Mamtimin, AIP Adv 10 (2020), 065330.
[53] S.F. Tayyari, F. Milani-nejad, Spectrochimica Acta Part A 56 (2000) 2679.
[54] B. Cohen, S. Weiss, J. Phys. Chem. 88 (1984) 3159.
[55] K.F. Herzfeld, T.A. Litovitz, Absorption and Dispersion of Ultrasonic Waves, Academic Press, New York, 1959 (b). J. Slutsky: Ultrasonic chemical relaxation spectroscopy, ed. P. D. Edmonds, Methods of Experimental Physics 19, Academic, New York, 1981, pp 179–235.
[56] M. Risva, P. Siafarika, A.G. Kalampounias, Physica B 630 (2022), 413697.
[57] A.G. Kalampounias, Chem. Phys. 561 (2022), 111618.
[58] A.G. Kalampounias, J. Molec. Struct. 1212 (2020), 128146.
[59] B. Jacobson, J. Chem. Phys. 20 (1952) 927.
[60] B. Jacobson, Acta Chem. Scand. 5 (1952) 485.
[61] R.A. Pethrick, Prog. Polym. Sci. 9 (1983) 197.
[62] U. Kaatze, T.O. Hushcha, F. Eggers, J. Solution Chem. 29 (2000) 299.
[63] M.M. Folkendt, B.E. Weiss-Lopez, J.P. Chauvel Jr, N.S. True, J. Phys. Chem. 89 (1985) 3347.
[64] P.Cabral do Couto, B.J.Costa Cabral, J.A. Martinho Simões, Chem. Phys. Lett. 419 (2006) 486.
[65] P. Roy, S. Biswas, A. Pramanik, P. Sarkar, Int. J. Res. Soc. Nat. Sci. 2 (2017) 2455.
[66] J.N. Spencer, E.S. Holmboe, M.R. Kirshenbaum, D.W. Firth, P.B. Pinto, Can. J. Chem. 60 (1982) 1178.
[67] L. Onsager, J. Amer, Chem. Soc. 58 (1936) 1486.
[68] J.G. Kirkwood, J. Chem. Phys. 4 (1936) 592.
[69] N.E. Hill, W.E. Vaughan, A.H. Price, M. Davies, Dielectric Properties and Molecular Behaviour, Van Nostrand Reinhold Company, London, 1969.
[70] G.G. Raju, Dielectrics in Electric Fields, Marcel Dekker, Inc., New York, 2003.
[71] A.K. Amirjahed, M.I. Blake, J. Pharm. Sci. 64 (1975) 1569.